Hindawi
Shock and Vibration
Volume 2021, Article ID 6631981, 10 pages
https://doi.org/10.1155/2021/6631981

Research Article

Numerical Simulation of Fine Particle Solid-Liquid Two-Phase Flow in a Centrifugal Pump

Yanping Wang ,[1] Bozhou Chen,[1] Ye Zhou ,[2] Jianfeng Ma,[3] Xinglin Zhang,[4] Zuchao Zhu,[1] and Xiaojun Li [1]

[1]*National-Provincial Joint Engineering Laboratory for Fluid Transmission System Technology, Zhejiang Sci-Tech University, Hangzhou 310018, China*
[2]*China Institute of Water Resources and Hydropower Research, Beijing 100038, China*
[3]*ZheJiang Fuchunjiang Hydropower Equipment Co., Ltd., Hangzhou 311501, China*
[4]*Hefei General Machinery Research Institute Co, Ltd, Hefei 230031, China*

Correspondence should be addressed to Ye Zhou; zhouye@foxmail.com and Xiaojun Li; lixj@zstu.edu.cn

Received 10 November 2020; Revised 24 January 2021; Accepted 8 February 2021; Published 18 February 2021

Academic Editor: Ling Zhou

To study the effect of fine particle size and volume concentration on the performance of solid-liquid two-phase centrifugal pump, the mixture multiphase flow model, RNG k-ε turbulence model, and SIMPLEC algorithm were used to simulate the two-phase flow of the centrifugal pump. The effects of particle size and volume concentration on internal pressure distribution, solid volume distribution, and external characteristics were analyzed. The results show that under the design discharge conditions, with the increase of particle size and volume concentration, the internal pressure of the flow field will decrease, and the volume fraction of solid phase in the impeller passage will also decrease as a whole. The solid particles gradually migrate from the suction surface to the pressure surface, and the particles in the volute channel are mainly concentrated in the flow channel near the outlet side of the volute. With the increase of particle size and volume concentration, the negative pressure value at the inlet of centrifugal pump increases, the total pressure difference at the inlet and outlet decreases, and the head and efficiency decrease accordingly.

1. Introduction

Solid-liquid two-phase centrifugal pump is one of the key power equipment for the hydraulic transport of solid-phase materials. It is widely used in various fields of national economy such as water conservancy engineering, petrochemical industry, marine metal mineral mining, and urban sewage treatment. The presence of solid particles makes the transport efficiency and reliability of this kind of centrifugal pump lower than that of the same structure of clean water pump. There have been a lot of numerical simulation and experimental research work at home and abroad at present [1–5], but most of the existing research focuses on the low concentration of solid-liquid two-phase flow and rarely involves the problem of dense fine particle solid-liquid two-phase flow. Up to now, the influence of dense fine particles on the flow field in centrifugal pump is still unclear, and the mechanism of dense fine particles solid-liquid two-phase centrifugal pump has not been revealed. Compared with the low concentration solid-liquid two-phase flow, the force of liquid and solid phase in high concentration solid-liquid two-phase flow is stronger [6–9]. The liquid-phase flow drives the movement of solid particles, and the loss of momentum and turbulent kinetic energy of solid particles in turn affects the liquid-phase flow. Particles collide with each other frequently, and the movement of particles is affected not only by the liquid phase in the pump, but also by the characteristics of particles. Therefore, it is of great significance to study the influence of particle size and volume concentration on the flow performance of centrifugal pump [10–13].

Due to the complexity of the solid-liquid two-phase flow in the centrifugal pump, the experimental research method is costly and time-consuming, and it is difficult to have a direct understanding of its internal flow state [14]. With the development of computational fluid dynamics, the experts at home and abroad have carried out in-depth research on solid-liquid two-phase flow in centrifugal pump based on the CFD method [15–18]. Liu et al. [19] used CFD technology to simulate the solid-liquid two-phase flow field in a chemical process pump, calculated the flow field in the pump under different particle sizes and concentrations, and studied the distribution of the solid-liquid two-phase flow of the double-suction pump. Li et al. [20] took a spiral centrifugal pump as the research object and analyzed the distribution and change rule of the initial solid-phase volume fraction along the internal flow field and its influence on the internal flow field of the spiral centrifugal pump. Zhang et al. [21] adopt the mixture model and moving grid technology to systematically study the influence of the properties of solid particles on the performance of centrifugal pump, including particle size, volume fraction, and density, and put forward the no-overload performance prediction of double channel pump and a calculation method that will substantial increase the accuracy in performance prediction. Cheng et al. [22] researched five different particle diameters and four different particle densities based on the particle model to study their influence on solid volume concentration distribution, solid-phase slip velocity, and external hydraulic characteristic in the double-blade sewage pumps. Liu et al. [23] calculated the unsteady flow field of solid volume fraction $C_v = 0\%$ and $C_v = 20\%$ in a multistage pump to analyze the influence of the addition of particles in the pump on its performance characteristic, and the distribution and movement of particles in impeller and guide vane are obtained at the same time. Song et al. [24] studied the internal and external characteristics of a vortex pump when the solid particle volume concentration is 5%, 10%, and 15%, and the results of the expression of pump head and efficiency are compared with the results of simulations.

At present, some progress has been made in numerical simulation of centrifugal pump flow performance [25–36]. However, the overall flow performance of the centrifugal pump, especially the two-phase flow performance under the condition of high concentration of fine particles, is not sufficiently studied due to the complexity of solid-liquid two-phase flow in the pump. On basis of the above research, the present study investigated a 1PN/4-3kw centrifugal pump to study the influence on the internal flow distribution in the pump for various particle size and volume concentration and to compare the results with the single-phase numerical simulation results of clean water. The results of this study are helpful to develop dense fine particle solid-liquid two-phase flow centrifugal pumps, improve transport efficiency, and reduce operating costs.

2. Computational Model and Mesh Generation

2.1. Model Parameters. 1PN/4-3 KW single-stage centrifugal pump was selected as the calculation model. The basic design parameters are as follows: flow $Q = 16\,\mathrm{m^3/h}$, head $H = 13\mathrm{m}$, and rotation $n = 1450\mathrm{r/min}$. The main geometrical parameters of the impeller are as follows: inlet diameter $d_1 = 50\,\mathrm{mm}$, outlet diameter $d_2 = 25\,\mathrm{mm}$, blade number $Z = 5$, the impeller is a semiopen impeller, the solid particles are glass beads, and $\rho = 2450\,\mathrm{kg/m^3}$. Unigraphics NX software was used to conduct 3D modeling of the pump, and the 3D model and hydraulic model of the centrifugal pump are shown in Figure 1.

2.2. Compute Domains and Grids. In order to make the numerical calculation results close to the real situation, an inlet extension section was added before the inlet of the suction chamber and an outlet extension section after the outlet of the volute respectively, so as to fully develop the water flow. The computational domain includes inlet extension section, impeller, volute, and outlet extension section. In order to improve the accuracy of simulation results, the unstructured mesh with good adaptability was used to grid the whole flow passage and the area with large pressure and velocity gradient was partially encrypted. A total of 6 grid schemes were set up to test and verify the grid's independence under steady flow of clean water at the centrifugal pump design condition, and the number of grids increased gradually from 1258424 to 4921565. The predicted head corresponding to different grid numbers is listed in Table 1, and the grid independence graph is shown in Figure 2. As it can be seen that the head is almost unchanged from the fourth grid, the calculated heads differed by less than 0.5%. Considering the computing performance of the computer, the fourth set of grid was chosen for the simulation, final overall mesh number of the model is 3,385,676, and the node number is 578,448. The calculation domain and mesh of the centrifugal pump are shown in Figure 3.

3. Mathematical Models and Boundary Conditions

3.1. The Basic Assumptions. The solid-liquid two-phase flow in the model pump is extremely complex. In order to simplify the calculation and improve the accuracy of the numerical simulation results, the following assumptions are adopted:

(1) The continuous phase (water) is an incompressible fluid, the particle phase is a continuous term, and the physical properties of each phase are constant
(2) The particle phase is a spherical glass bead with uniform particle size, regardless of the change of particle shape
(3) Internal flow of the pump is treated as steady flow with water as principle phase, solid particle as secondary phase
(4) Axial velocity of inlet is well-distributed, and solid particles and water are evenly mixed with same velocity

3.2. Multiphase Flow Model. Considering the interaction between solid and liquid phases, because the particle size is small (≤1 mm), solid particles can be treated as a continuous

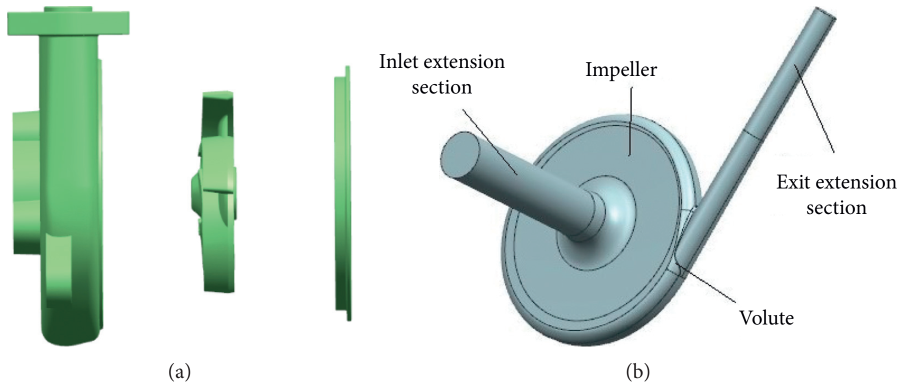

FIGURE 1: 3D model and hydraulic model of centrifugal pump: (a) 3D model of centrifugal pump; (b) hydraulic model of centrifugal pump.

TABLE 1: Predicted head with various grids.

Scheme	1	2	3	4	5	6
Grid number	1,258,424	1,648,573	2,324,618	3,385,676	4,025,178	4,921,565
Head	14.58	14.32	13.83	13.69	13.65	13.70

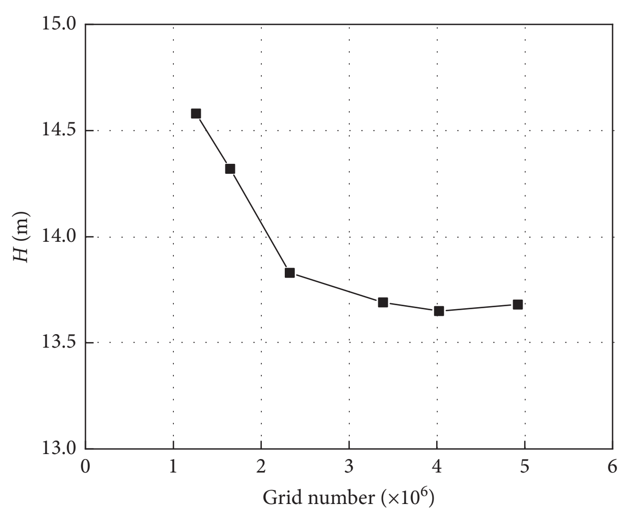

FIGURE 2: Grid independence graph.

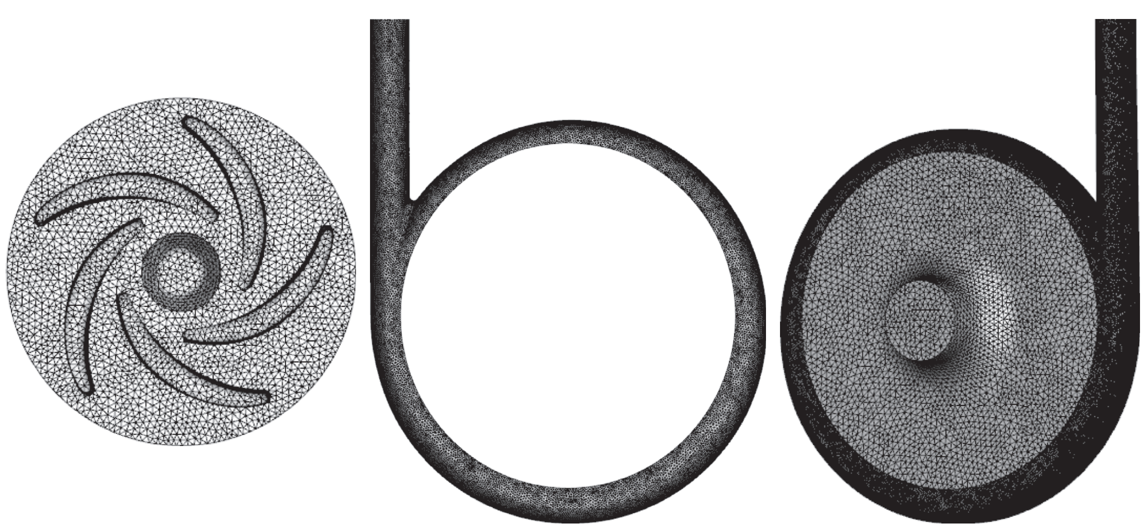

FIGURE 3: Calculation domain and grid of centrifugal pump.

medium, and the phase coupling is quite strong. Therefore, the mixture model is adopted, and its continuity equation and momentum equation are as follows.

Continuity equation:

$$\frac{\partial}{\partial t}(\rho_m) + \nabla \cdot (\rho_m \vec{v}_m) = 0. \quad (1)$$

Among them, ρ_m is the mixture density, kg/m^3, and $\vec{v}_m$ is the average mass velocity, m/s.

Momentum equation:

$$\begin{aligned}\frac{\partial}{\partial t}(\rho_m \vec{v}_m) + \nabla \cdot (\rho_m \vec{v}_m \vec{v}_m) \\ = -\nabla p + \nabla \cdot \left[\mu_m\left(\nabla \vec{v}_m + \nabla \vec{v}_m^T\right)\right] + \rho_m \vec{g}_m + \vec{F} \\ + \nabla \cdot \left(\sum_{k=1}^{n} \alpha_k \rho_k \vec{v}_{dr,k} \vec{v}_{dr,k}\right).\end{aligned} \quad (2)$$

Among them, μ_m is the coefficient of mixing viscosity, Pa·s; $\vec{F}$ is the volume force, N; n is the number of phase; α_k is the volume fraction of the k^{th} term, %; ρ_k is the k^{th} density, kg/m^3; and $\vec{v}_{dr,k}$ is the k^{th} term drift velocity, m/s.

Slip velocity $\vec{v}_{qp}$ is defined as the velocity of the second phase (p) relative to the main phase (q):

$$\vec{v}_{qp} = \vec{v}_p - \vec{v}_q. \quad (3)$$

Then, the relationship between drift velocity and slip velocity is

$$\vec{v}_{dr,p} = \vec{v}_{qp} - \sum_{k=1}^{n} \frac{\alpha_k \rho_k}{\rho_m} \vec{v}_{qk}. \quad (4)$$

From the continuity equation of the second phase (p), the volume fraction equation of the second phase can be obtained as follows:

$$\frac{\partial}{\partial t}\left(\alpha_p \rho_p\right) + \nabla \cdot \left(\alpha_p \rho_p v_m\right) = -\nabla \cdot \left(\alpha_p \rho_p v_{dr,p}\right). \quad (5)$$

3.3. Boundary Conditions. The RNG k-ε turbulence model was used to simplify and close the equations. The SIMPLEC algorithm was used for numerical solution, and the convergence accuracy was set as 10^{-6}. The inlet boundary condition adopts the velocity inlet, only considers the axial velocity, and does not consider the fluid or particle moving in other directions, and it can be obtained according to the design flow rate and inlet pipe diameter. The outlet boundary condition chooses the free flow outlet, and the inlet and outlet turbulence intensity is consistent with the default value of 5%. The impeller wall is set to rotate, the other walls are static, the boundary condition of the wall is no slip condition, and the standard wall function is adopted near the wall.

The particle diameter was adjusted by defining the solid-phase parameters in the mixed model, and the volume concentration was achieved by setting the inlet solid-phase volume fraction in the boundary conditions.

4. Calculation Results and Analysis

In order to explore the influence of particle size and volume concentration on centrifugal pump performance during solid-liquid two-phase flow transportation, the following calculation scheme is formulated:

(1) At the design flow rate and the solid-phase concentration of 10%, the two-phase flow field under five working conditions with particle size of 0.01 mm, 0.05 mm, 0.1 mm, 0.15 mm, and 0.2 mm was numerically simulated

(2) At the designed flow rate and the particle size of 0.1 mm, the two-phase flow field under five working conditions with particle concentration of 10%, 15%, 20%, 25%, and 30% s was numerically simulated

4.1. External Characteristics of Centrifugal Pump When Conveying Clean Water. Firstly, numerical simulation was carried out for the external characteristics of the centrifugal pump when transporting clean water and the numerical simulation results were compared with the test results, as shown in Figure 4. It can be seen that the flow-head curve trend of the numerical simulation and the test is basically the same, and the head of the numerical simulation is higher than that of the test, because the simulation value does not take the error factors caused in the casting process of the centrifugal pump into account, such as the surface roughness of the impeller and volute. The flow-efficiency curve of the numerical simulation is also consistent with the variation trend of the test value. When the flow is close to the working point, there is little difference between them. The maximum error between the numerical calculation and pump test results is less than 8%; therefore, it is reasonable to believe that the model and method adopted in the numerical simulation of two-phase flow of the test pump are reasonable.

4.2. Influence of Particle Size on Internal Flow Performance. Figure 5 shows the cloud diagram of centrifugal pump pressure distribution with different particle sizes when $C_v = 10\%$. It can be seen from the figure that the final pressure cloud map changes little after different small-size particles are input into the flow passage of the centrifugal pump while the volume fraction is fixed. The pressure at the inlet of the flow passage is negative, and it can be analyzed that the particles at the inlet collide with each other, leading to the decrease of the pressure, and the negative pressure will lead to the cavitation of the centrifugal pump. As the particle size increases, the chance of collision also increases, which aggravates the negative pressure and finally leads to the continuous decline of the cavitation performance of the centrifugal pump. The pressure of the impeller passage is not completely symmetrical and consistent. The pressure near the outlet pipe of the volute is larger than that of other parts. After careful observation, it was found that the pressure at the position close to the outlet pipe in the condition of 0.01 mm particle size was higher than that of 0.2 mm.

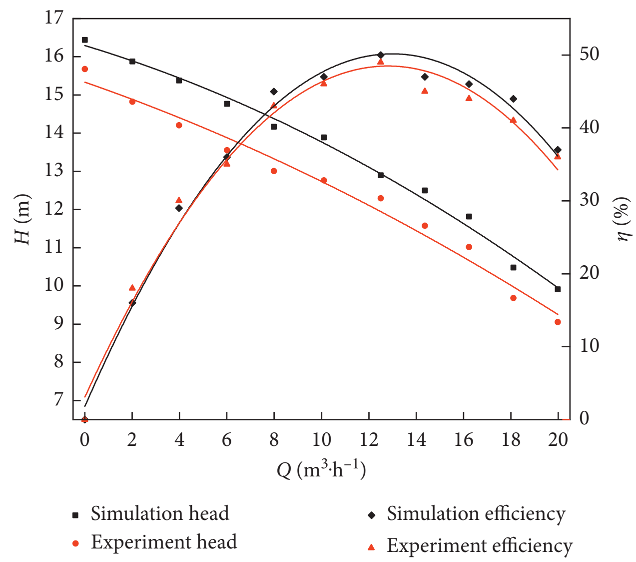

Figure 4: Verification of external characteristics of centrifugal pump.

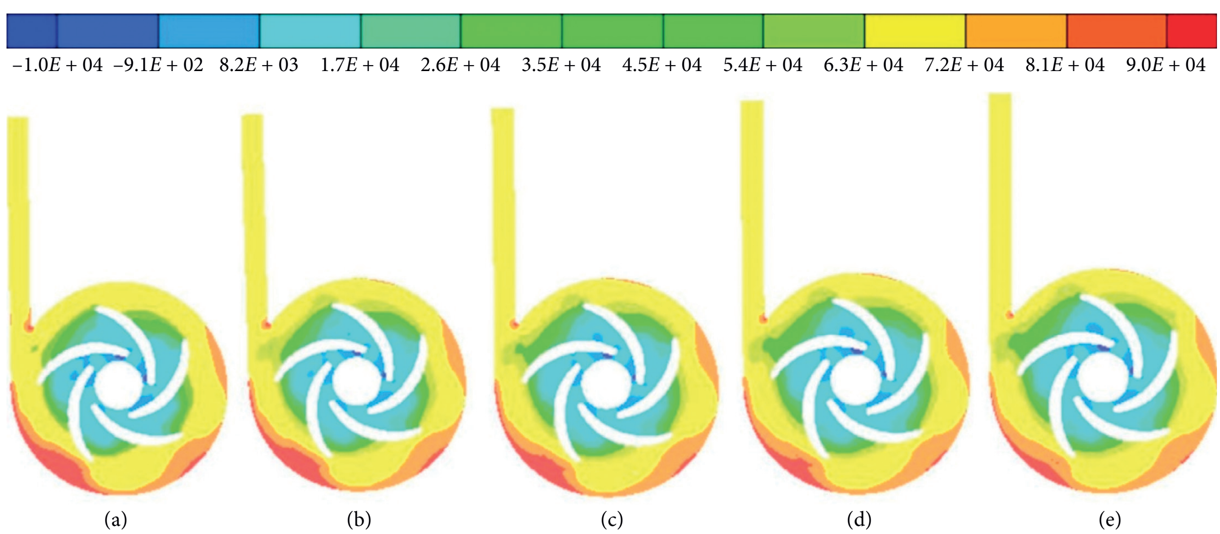

Figure 5: Cloud diagram of centrifugal pump pressure with different particle sizes ($C_v = 10\%$): (a) 0.01 mm, (b) 0.05 mm, (c) 0.1 mm, (d) 0.15 mm, and (e) 0.2 mm.

Therefore, it was speculated that as the particle size increased, the overall pressure inside the flow field tended to decrease.

As the particle size increases, the pressure changes little in the impeller passage, but after the two-phase flow enters the pressure chamber, the pressure begins to change obviously, especially the pressure along the volute wall generally decreases. It can be seen that the pressure changes little at the impeller inlet but decreases obviously at the volute outlet, and the pressure changes very sharply on both sides of the tongue. Because the fluidity of solid particles decreases as the particle size increases, the energy consumed by conveying particles increases, resulting in the continuous drop of total pressure in the pump. The macroscopic manifestation is that the efficiency of centrifugal pump gradually decreases and the head decreases gradually.

Figure 6 shows the liquid-phase velocity distribution in the middle section. The velocity increases gradually from the impeller inlet to outlet. At the same radial distance, the relative velocity at the pressure side of the blade is lower than that at the suction side in the latter part of blade. With the change of particle size, the liquid velocity distribution has little change. The high-speed region appears near the back side of the impeller outlet, and there is wake at the outlet of the impeller channel.

As the particle size increases, the wake area of impeller gradually increases, the high-speed region near the tongue increases, and the low-speed region at the outlet of volute increases. This is because when the particle size increases, the flow performance of particles decreases, the particle concentration near the back of the impeller decreases, the relative liquid concentration increases, thus cause the range

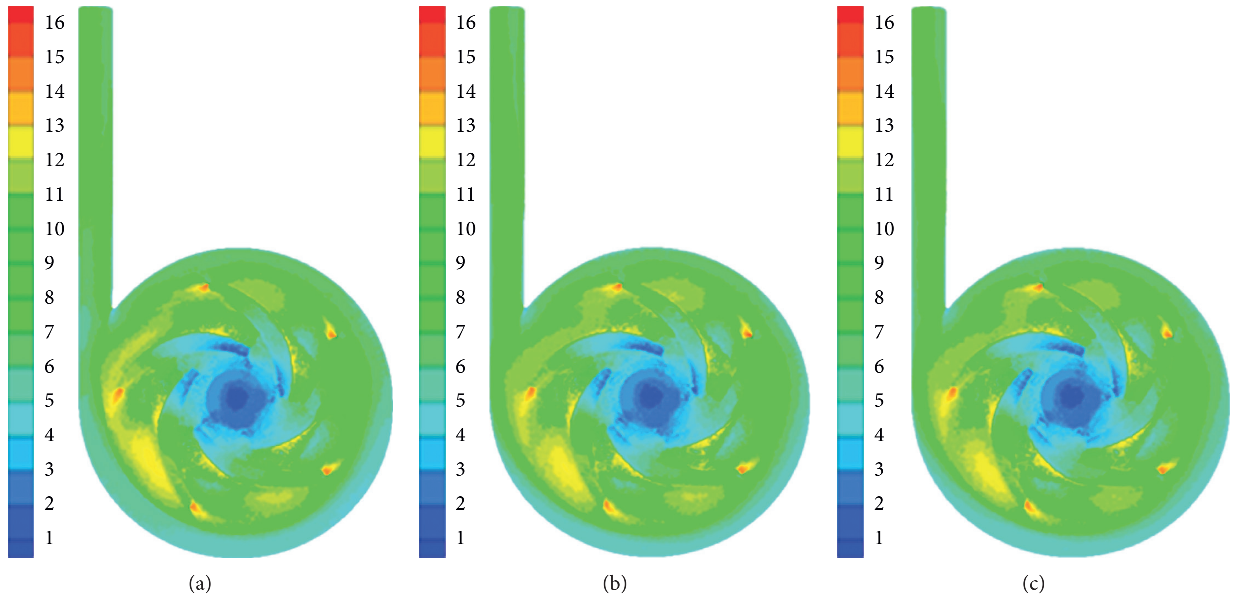

FIGURE 6: Cloud diagram of centrifugal pump velocity with different particle sizes ($C_v = 10\%$): (a) 0.01 mm, (b) 0.1 mm, and (c) 0.2 mm.

of high-speed region near the back side of the impeller increases gradually. As the particle size increases, the number of particles reflux into the impeller channel from the tongue decreases, the concentration of the liquid phase increases, and the range of the high-speed zone gradually increases, indicating that the size of the particle has a serious impact on the reflux near the tongue.

Figure 7 shows the cloud diagram of solid-phase volume distribution of centrifugal pump impeller with different particle sizes when $C_v = 10\%$. It can be seen from the figure that the distribution trend of particle volume concentration of different particle sizes is consistent. Since the inlet boundary condition is set with the same initial velocity, the solid-phase volume concentration distribution is relatively uniform near the impeller inlet. As the flow progresses, the impeller takes effect and the solid volume concentration distribution changes. With the increase of particle size, the concentration of solid particles on the pressure surface of impeller is significantly higher than that on the suction surface, and the volume concentration of solid particles in impeller channel decreases as a whole. The reason is that with the increase of particle size, the centrifugal force of the impeller increases, and the solid particles deviate from the suction surface of the impeller and move towards the pressure surface.

As the particle size increases, the particle concentration at the head of the blade working face increases, and the particle concentration at the back of the blade decreases along the direction of the impeller passage. When the particle size is 0.01 mm, the concentration distribution on the blade is relatively average. From the inlet to the outlet of the impeller, the particle concentration on the working surface at the inlet is higher, decreases along the impeller passage and increases along the back of the blade. As the particle size increases, the particle concentration at the inlet of the blade-working face increases, and the particle concentration at the back side decreases. When the particle size is 0.2 mm, it can be clearly seen that the particle concentration distribution on the back side of the blade is extremely uneven. The larger the particle size is, the greater the inertia force on the particle is, and the more obvious the migration from the working face to the back is. Therefore, it is concluded that the particle diameter has a great influence on the overall concentration distribution of the working face and the back side of the blade.

4.3. Influence of Volume Concentration on Internal Flow Performance. Figure 8 shows the pressure distribution cloud diagram of centrifugal pump with different solid-phase volume concentrations at $d = 0.1$ mm. It can be found from the figure that the influence of the change of volume concentration on the pressure of the full flow passage in the centrifugal pump is similar to that of the change of particle size. When the particle size is fixed, with the increase of solid volume concentration, the negative pressure at the inlet of the impeller increases, the possibility of cavitation increases, the pressure difference between pump inlet and outlet decreases, and the head of the centrifugal pump decreases.

As the particle volume fraction increases, the negative pressure at the impeller inlet gradually increases, and the negative pressure mainly distributes on the suction surface of the blade head. The volute diameter changes the most at the tongue, so the pressure changes obviously here. When conveying the mixed medium, the influence of particle volume fraction on the inlet and outlet of the pump and near wall area of the volute is relatively large. With the increase of the volume fraction of particles, the collisions between particles and the wall become more frequent, and the average density of the fluid increases. Therefore, the more energy is needed to transport the mixed medium, which leads to the increasing negative pressure at the inlet and outlet of the impeller and the increasing total pressure in the pump.

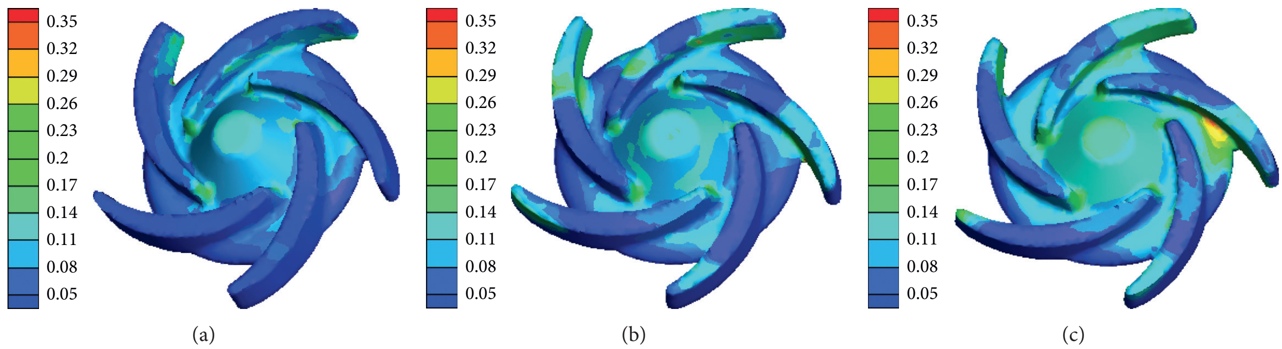

Figure 7: Cloud diagram of solid-phase volume distribution of impeller with different particle sizes ($C_v = 10\%$): (a) 0.01 mm, (b) 0.1 mm, and (c) 0.2 mm.

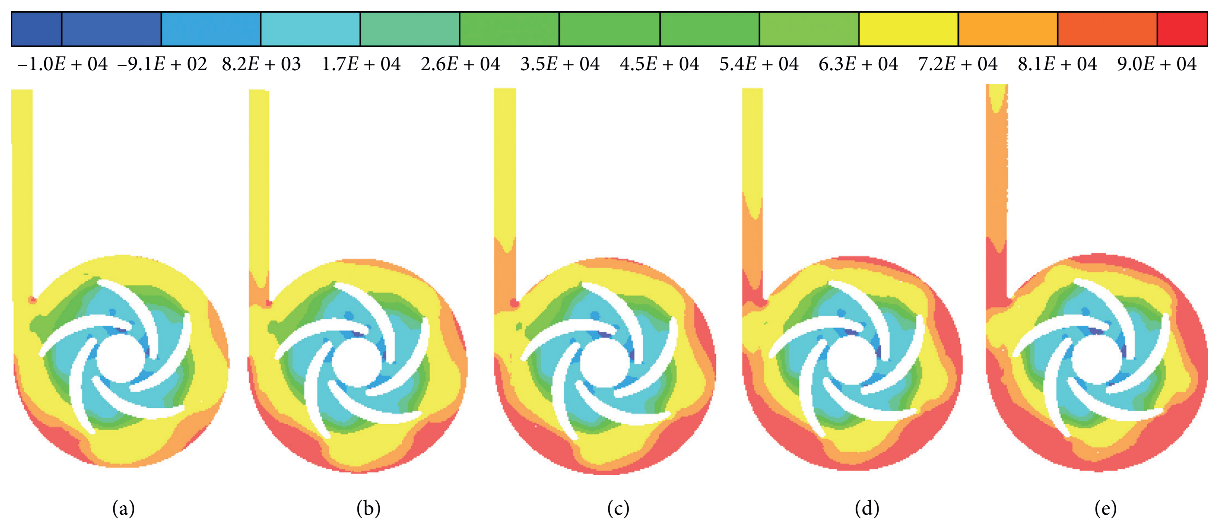

Figure 8: Cloud diagram of centrifugal pump pressure at different concentrations ($d = 0.1$ mm): (a) $C_v = 10\%$, (b) $C_v = 15\%$, (c) $C_v = 20\%$, (d) $C_v = 25\%$, and (e) $C_v = 30\%$.

It can be seen from Figure 9 that the liquid-phase velocity along the impeller channel increases gradually, and the smaller the volute diameter is, the greater the velocity is. There is a high-speed area near the tongue, and a high-speed area appears near the back side of the impeller outlet.

As the particle volume fraction increases, the liquid velocity at the impeller outlet increases obviously, and the high-speed region in the water pressure chamber is mainly located at the position with small volute diameter. On the whole, the change of particle volume fraction does not affect the distribution of liquid velocity, indicating that the particle volume fraction has little effect on the liquid velocity.

Figure 10 shows the cloud diagram of solid-phase volume distribution of centrifugal pump impeller with different volume concentrations at $d = 0.1$ mm. It can be seen from the figure that during the movement of particles from the inlet to the outlet, the solid-phase volume concentration on the suction surface of the blade is significantly higher than that on the pressure surface. With the increase of initial concentration of solid-phase volume, the particles tend to move towards the pressure surface, $C_v = 10\%$, the particle at a certain inlet angle into the impeller flow channel, and the back part of the particle impact blade, with the deepening of the flow, under the action of inertial force to be near blade pressure side; with the increase of volume concentration, the impact on the back of the trend gradually disappears, and that solid-phase volume concentration has a certain influence on particle size distribution.

The particle concentration along the back of the volute first decreases and then increases, and the range of particle concentration decreases gradually to the blade tail with the increase of the volute diameter. In the area near the wall of the volute, the particle concentration gradually increases with the increase of the volute diameter, and the particle concentration is the highest at the maximum volute diameter; the particle concentration is generally higher at the head of impeller working face and the tail wake of blade back. With the increase of particle volume fraction, the particle concentration in the impeller increases gradually, but the overall distribution remains unchanged, which indicates that the change of particle volume fraction only affects the particle concentration in the pump but does not affect the overall distribution of particles in the pump.

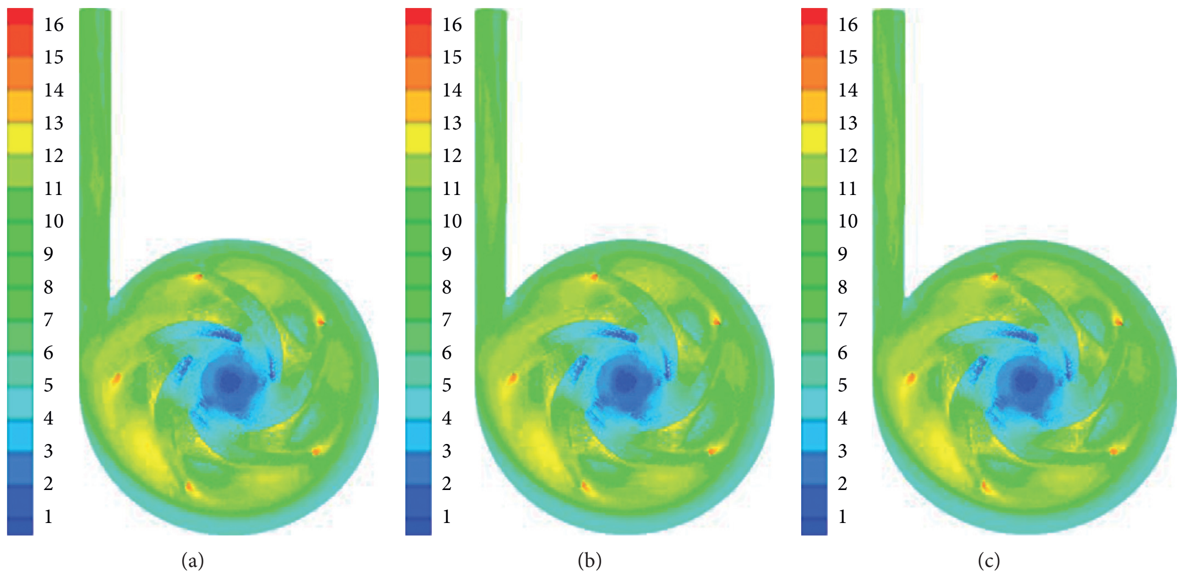

Figure 9: Cloud diagram of centrifugal pump velocity at different concentrations ($d = 0.1$ mm): (a) $C_v = 10\%$, (b) $C_v = 20\%$, and (c) $C_v = 30\%$.

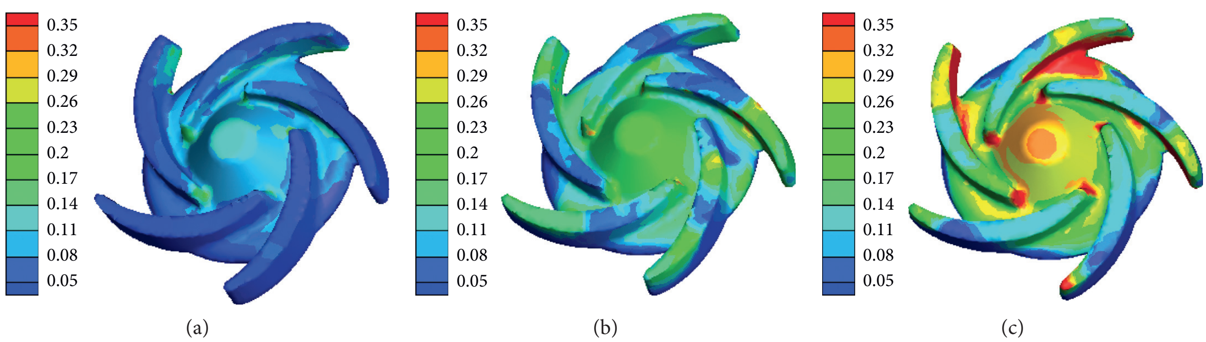

Figure 10: Cloud diagram of solid-phase volume distribution of impeller of different concentrations ($d = 0.1$ mm): (a) $C_v = 10\%$, (b) $C_v = 20\%$, and (c) $C_v = 30\%$.

4.4. Effects of Solid Particles on Pump Characteristics. In this paper, the internal flow field of the centrifugal pump with particle diameter of 0.01 mm, 0.05 mm, 0.1 mm, 0.15 mm, and 0.2 mm and volume concentration of 10%, 15%, 20%, 25%, and 30% under the design flow condition was simulated. The influence of particle diameter and volume concentration on the head and efficiency of the centrifugal pump was analyzed through the simulation results. In order to express the calculation results more intuitively, it is shown in the chart form as follows.

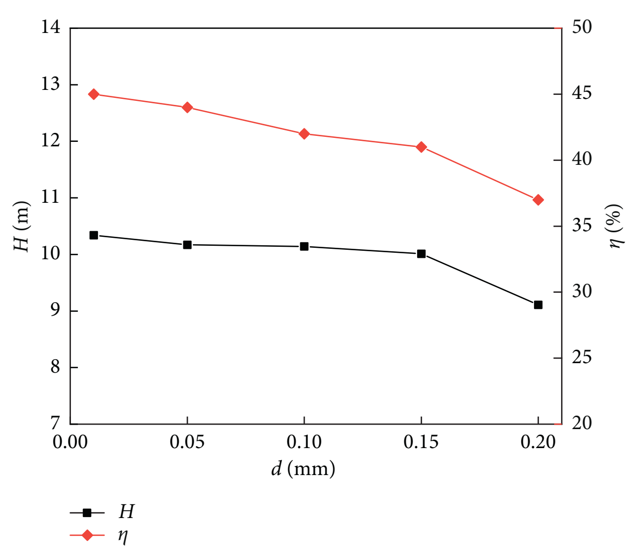

Figure 11: Influence of particle size on head and efficiency.

Figure 11 shows that the head and efficiency of the centrifugal pump decrease with the increase of particle diameter. When the particle diameter is less than 0.15 mm, the particle diameter has little influence on the head and certain influence on the efficiency. When the particle diameter is larger than 0.15 mm, the head and efficiency decrease significantly. It can be seen that the particle size of the solid phase suitable for transport by this model pump is smaller than 0.15 mm. The reason for the decline of hydraulic

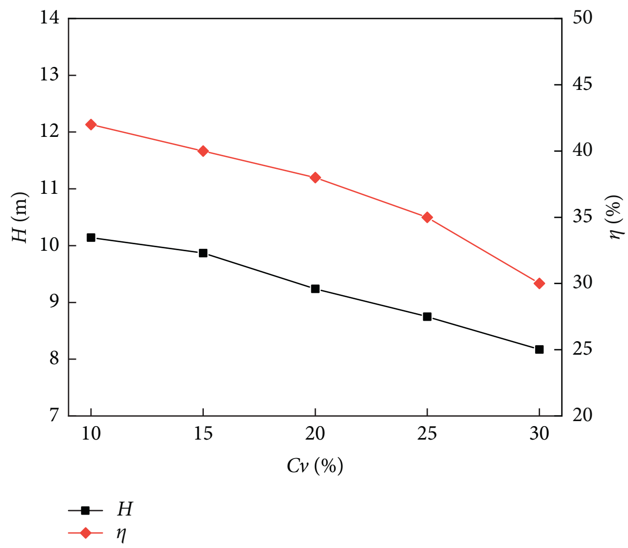

Figure 12: Influence of volume concentration on head and efficiency.

performance may be as follows: with the increase of particle diameter, the greater the energy needed to maintain the suspension drifting in the flow, the more serious the hydraulic loss will be, leading to the deterioration of external characteristics.

It can be seen from Figure 12 that, under the same particle diameter condition, the head and efficiency of the centrifugal pump significantly decrease with the increase of the solid-phase volume concentration, and the change trend is approximately linear. The reason for the decline of hydraulic performance may be that with the increase of the volume concentration of solid phase, the viscosity of the solid-liquid mixture increases, the probability of collision between particles also increases greatly, and the hydraulic loss worsens, resulting in the decline of external characteristic performance.

5. Conclusions

The mixture multiphase flow model, the extended RNG k-ε turbulence model, and SIMPLEC algorithm were used for numerical simulation of solid-liquid two-phase turbulence in a centrifugal pump using the fluid dynamics software Fluent:

(1) With the particle size increases, the negative pressure at the inlet of the impeller intensifies, and the impeller runner pressure is not completely symmetrical and consistent. The pressure near the outlet pipe of the volute is large, and the overall pressure inside the flow field decreases. The solid-phase volume concentration in the impeller passage decreases as a whole, and the solid particles tend to migrate away from the suction of the impeller towards the pressure surface due to the centrifugal force of the impeller.

(2) With the increase of solid-phase volume concentration, similar to the influence of particle size change on pressure, the negative pressure at the inlet of impeller increases, the possibility of cavitation in the pump increases, and the pressure at the outlet decreases. The solid-phase volume concentration on the suction surface of the blade is higher than that on the pressure surface. With the increase of the initial solid-phase volume concentration, the particles also tend to move towards the pressure surface.

(3) Under the design flow condition, with the increase of particle size and volume concentration, the negative pressure value at the inlet of the centrifugal pump increases, the total pressure difference at the inlet and outlet decreases, and the head and efficiency decrease accordingly.

Data Availability

The data used to support the findings of this study are available from the corresponding author upon request.

Conflicts of Interest

The authors declare that they have no conflicts of interest.

Acknowledgments

The authors thank the National Natural Science of China (grant no. 51676174) and Key Research and Development Program of Zhejiang Province (grant no. 2020C1027) for the financial support.

References

[1] Y. Yang, L. Zhou, W. Shi, Z. He, Y. Han, and Y. Xiao, "Interstage difference of pressure pulsation in a three-stage electrical submersible pump," *Journal of Petroleum Science and Engineering*, vol. 196, Article ID 107653, 2021.

[2] S. H. Liu, X. L. Tang, and Y. L. Wu, "Simulation of dense solid-liquid two-phase flow in a pump impeller," in *Proceedings of the ASME 2004 Heat Transfer/Fluids Engineering Summer Conference*, no. 2, pp. 461–467, Charlotte, CA, USA, July 2004.

[3] D. Liu and M. G. Yang, "Research of liquid-solid two phase flow in the chemical pump," *Advances in Water Resources and Hydraulic Engineering*, vol. 7, p. 2203, 2009.

[4] J. R. Liu, Y. G. Xu, and D. M. Wang, "Analysis of liquid-solid two-phase Turbulent Flow in FGD system pump," in *Proceedings of the 2009 IEEE 10th International Conference on Computer-Aided Industrial Design & Conceptual Design*, Wenzhou, China, November 2009.

[5] T. Lin, Z. Zhu, X. Li, J. Li, and Y. Lin, "Theoretical, experimental, and numerical methods to predict the best efficiency point of centrifugal pump as turbine," *Renewable Energy*, vol. 168, no. 5, pp. 31–44, 2021.

[6] A. Amoresano, G. Langella, V. Niola, and G. Quaremba, "Advanced image analysis of two-phase flow inside a centrifugal pump," *Advances in Mechanical Engineering*, vol. 6, no. 1, pp. 958320–958700, 2014.

[7] B. Shi and J. Wei, "Numerical simulation of 3D solid-liquid turbulent flow in a low specific speed centrifugal pump: flow field analysis," *Advances in Mechanical Engineering*, vol. 6, no. 2, Article ID 814108, 2014.

[8] B. Wu, X.-L. Wang, H. Liu, and H.-L. Xu, "Numerical simulation and analysis of solid-liquid two-phase three-

dimensional unsteady flow in centrifugal slurry pump," *Journal of Central South University*, vol. 22, no. 8, pp. 3008–3016, 2015.

[9] S. Huang, X. Su, G. Qiu et al., "Transient numerical simulation for solid-liquid flow in a centrifugal pump by DEM-CFD coupling," *Engineering Applications of Computational Fluid Mechanics*, vol. 9, no. 1, pp. 411–418, 2015.

[10] C. Shao, J. Zhou, W. Cheng et al., "Experimental and numerical study of external performance and internal flow of a molten salt pump that transports fluids with different viscosities," *International Journal of Heat and Mass Transfer*, vol. 89, pp. 627–640, 2015.

[11] P. K. Gupta, "Role of centrifugal force on solid-liquid two-phase flow through rotating channel," *Progress in Computational Fluid Dynamics, An International Journal*, vol. 17, no. 5, pp. 326–331, 2017.

[12] C. Ning and Y. Wang, "Performance analysis on solid-liquid mixed flow in a centrifugal pump," *IOP Conference Series: Materials Science and Engineering*, vol. 129, Article ID 012062, 2016.

[13] L. Wang, B. Li, and W. Zhao, "Dynamics and wear analysis of hydraulic turbines in solid-liquid two-phase flow," *Open Physics*, vol. 17, no. 1, pp. 790–796, 2019.

[14] J. H. Liu and M. Y. Zhu, "Numeration simulation of solid-liquid two-phase flow in centrifugal sewerage pump," *Applied Mechanics and Materials*, vol. 44–47, pp. 345–348, 2010.

[15] B. J. Zhao, Z. F. Huang, H. L. Chen, and D. H. Hou, "Numerical investigation of solid-liquid two phase flow in a non-clogging centrifugal pump at off-design conditions," *IOP Conference Series: Earth and Environmental Science*, vol. 15, Article ID 062020, 2012.

[16] H. Hua, X. B. Liu, S. B. Ou, and Y. Z. Zeng, "Numerical simulation of 3D solid-liquid two-phase turbulence flow in axial-flow pump impeller," *Applied Mechanics and Materials*, vol. 212-213, pp. 1237–1243, 2012.

[17] H. Hua, X. L. Wang, H. Y. Wang et al., "Analysis of solid-liquid two-phase flow in axial flow pump," *Applied Mechanics and Materials*, vol. 229–231, pp. 559–564, 2012.

[18] Y. Li, Z. Zhu, W. He, and Z. He, "Numerical simulation and experimental research on the influence of solid-phase characteristics on centrifugal pump performance," *Chinese Journal of Mechanical Engineering*, vol. 25, no. 6, pp. 1184–1189, 2012.

[19] Y. Liu, Y. Jiang, and Z. J. Han, "Research on the pattern of solid-liquid two-phase distribution in chemical process pump," *IOP Conference Series: Earth and Environmental Science*, vol. 15, Article ID 072009, 2012.

[20] R. N. Li, H. Y. Wang, W. Han, W. Ma, and Z. J. Shen, "Study on solid-liquid two-phase unsteady flow characteristics with different flow rates in screw centrifugal pump," *IOP Conference Series: Materials Science and Engineering*, vol. 52, Article ID 062002, 2013.

[21] Y. Zhang, Y. Li, B. Cui, Z. Zhu, and H. Dou, "Numerical simulation and analysis of solid-liquid two-phase flow in centrifugal pump," *Chinese Journal of Mechanical Engineering*, vol. 26, no. 1, pp. 53–60, 2013.

[22] C. Cheng, W. D. Shi, D. S. Zhang et al., "Numerical simulation of solid-liquid two-phase turbulent flow in swept-back sewage centrigual pump," in *Proceedings of the 2014 ISFMFE-6th International Symposium on Fluid Machinery and Fluid Engineering*, Wuhan, China, October 2014.

[23] G. H. Liu, W. D. Cao, Y. Li et al., "Study on solid-liquid two-phase unsteady flow in multistage pump," in *Proceedings of the 2014 ISFMFE-6th International Symposium on Fluid Machinery and Fluid Engineering*, Wuhan, China, October 2014.

[24] P. Y. Song, H. L. Wang, and P. C. He, "The numerical simulation and performance analysis of the vortex pump for solid-liquid two phase medium," *Applied Mechanics and Materials*, vol. 527, pp. 88–92, 2014.

[25] Z. J. Shen, R. N. Li, W. Han, W. G. Zhao, and X. H. Wang, "The research on particle trajectory of solid-liquid two-phase flow and erosion predicting in screw centrifugal pump," *IOP Conference Series: Materials Science and Engineering*, vol. 129, Article ID 012052, 2016.

[26] W. Cheng, B. Gu, C. Shao, and Y. Wang, "Hydraulic characteristics of molten salt pump transporting solid-liquid two-phase medium," *Nuclear Engineering and Design*, vol. 324, pp. 220–230, 2017.

[27] Y. Gu, N. Liu, J. Mou, P. Zhou, H. Qian, and D. Dai, "Study on solid-liquid two-phase flow characteristics of centrifugal pump impeller with non-smooth surface," *Advances in Mechanical Engineering*, vol. 11, no. 5, Article ID 1687814019848269, 2019.

[28] S. J. Huang and C. L. Shao, "Solid-liquid two-phase flow characteristics in centrifugal pump with multi-component medium," *Transactions of the Chinese Society of Agricultural Engineering*, vol. 32, no. 20, pp. 77–84, 2016.

[29] R. Tarodiya and B. K. Gandhi, "Numerical simulation of a centrifugal slurry pump handling solid-liquid mixture: effect of solids on flow field and performance," *Advanced Powder Technology*, vol. 30, no. 10, pp. 2225–2239, 2019.

[30] L. Bai, L. Zhou, C. Han, Y. Zhu, and W. Shi, "Numerical study of pressure fluctuation and unsteady flow in a centrifugal pump," *Processes*, vol. 7, no. 6, p. 354, 2019.

[31] G. Peng, X. Huang, L. Zhou, G. Zhou, and H. Zhou, "Solid-liquid two-phase flow and wear analysis in a large-scale centrifugal slurry pump," *Engineering Failure Analysis*, vol. 114, Article ID 104602, 2020.

[32] S. Kebriti and H. Moqtaderi, "Numerical simulation of convective non-Newtonian power-law solid-liquid phase change using the lattice Boltzmann method," *International Journal of Thermal Sciences*, vol. 159, Article ID 106574, 2021.

[33] D.-S. Zhang, Q. Pan, Z. Hu, W.-D. Shi, R.-J. Zhang, and J. Xing, "Numerical simulation and optimization of solid-liquid two-phase flow in a back-swept axial-flow pump," *Thermal Science*, vol. 21, no. 4, pp. 1751–1757, 2017.

[34] X. Y. Xing and Y. J. Xu, "The numerical and experimental research on solid-liquid two-phase flow pattern in the PID," *Advances in Petroleum Exploration and Development*, vol. 9, no. 2, pp. 111–116, 2015.

[35] Y. Zhang, Y. Li, Z. Zhu, and B. Cui, "Computational analysis of centrifugal pump delivering solid-liquid two-phase flow during startup period," *Chinese Journal of Mechanical Engineering*, vol. 27, no. 1, pp. 178–185, 2014.

[36] X. L. Tang, S. Y. Yang, F. J. Wang, and Y. L. Wu, "Numerical investigations of solid-liquid two-phase turbulent flows through francis turbine," *Advanced Materials Research*, vol. 548, pp. 853–859, 2012.